EasyChair Preprint

№ 6700

Design of a Medium-Scale Circulating Fluidized Bed Reactor for Chlorination of Processed Aluminum Oxide

Zahir Barahmand, Omid Aghaabbasi, Jose Luis Salcido, Emmy Kristine Rustad, Chameera Jayarathna and Chandana Ratnayake

September 26, 2021

Design of a Medium-Scale Circulating Fluidized Bed Reactor for Chlorination of Processed Aluminum Oxide

Zahir Barahmand[1] Omid Aghaabbasi[1] Jose Luis Salcido[1] Emmy Kristine L. Rustad[1]
Chameera Jayarathna[2] Chandana Ratnayake[1,2]

[1] Department of Process, Energy and Environmental Technology, University of South-Eastern Norway
zbarahmand@gmail.com
[2] SINTEF Tel-Tek, SINTEF Industry, Porsgrunn, Norway

Abstract

Fluidization is a well-established and widely used technology in the process industry. The production stability and the large effective contact area between the active substances, resulting in high mass and heat transfer between the phases, are some of the main advantages of fluidization. However, this technology has not yet been adequately developed for alumina chlorination as a standard solution on an industrial scale. Although a circulating fluidized bed reactor design is complex by its nature, it is advantageous to simulate the process compared to running experiments on a lab scale. The Computational Particle-Fluid Dynamic (CPFD) simulation lays a foundation for studying the given reaction process.

The reaction between the solid alumina particles and the gaseous chlorine and carbon monoxide results in the products (aluminum chloride and carbon dioxide). The present study aims to design a circulating fluidized bed reactor by simulating the process in Barracuda®. Simulations with a simple geometry contributed to a better understanding of the reaction process. Then the simulation results are compared with values from both a theoretical approach and parallel simulations in Aspen Plus®. The comparison revealed that the results from Barracuda® Virtual Reactor (VR), such as product flow rate, are within a reasonable range of what could be expected in a full-scale plant. The promising preliminary results imply that CPFD could be a promising approach for future research on the design, optimization, and implementation of the industrial alumina chlorination process. The final design includes a fluidized bed reactor with a 2.4 m internal diameter and 8 m height and four parallel internal cyclones on top.

Keywords: CPFD Simulation, Alumina Chlorination, Circulating Fluidized Bed Reactor (CFBR), Reactor Design, Barracuda, Fluidization, Multiphase flow

1 Introduction

The earth's crust is rich in aluminum. It can only be found in mineral compositions, for example, alumina-silicates, clays, and hydrated oxides like bauxite. Producing aluminum from bauxite is mainly done by extraction in a Bayer process (Survey of Potential Processes for the Manufacture of Aluminium, 1979). This is done by dissolving alumina with soda ash and lime in steel digesters and converting it to pure aluminum by an electrochemical process, namely Hall-Héroult (Thonstad, 2001). This process has a considerable power requirement and greenhouse gas (GHG) emissions. Because of that, it is important to evaluate an alternative process. The challenge lies in finding a proper and economical solution, considering the complexity of alumina's carbothermic reduction (Rao & Soleiman, 1986). Even if alumina is pure, the result is aluminum metal and aluminum carbide. This again needs to decompose carbide to metal at 2100°C.

The solution could be a two-step process that converts alumina to aluminum chloride ($AlCl_3$) and then reduces it to metal aluminum. At first, it was suggested to reduce $AlCl_3$ with manganese, but it was not an excellent economical choice (*Survey of Potential Processes for the Manufacture of Aluminum*, 1979). Alcoa® proposed a solution for this second step as the electrolysis of $AlCl_3$ with alkali and alkaline earth chlorides (Rhamdhani et al., 2013). This solution appears to be a more economical and energy-saving method. Current research and development study has been focusing on producing aluminum chloride from alumina.

One proposed technology for the chlorination of alumina is a fluidized bed reactor (National Fuels and Energy Conservation Act, 1973). This technology has a wide range of possible applications. The upward flow of a fluid through a bed of solid particles is a technique that results in an efficient heat and mass transfer and generally offers a stable and efficient production. The challenge of using a Circulating Fluidized Bed (CFB) reactor lies in the design of the reactors due to the complexity of the flow patterns and the flow dynamics with multiphase situations within the reactors. This makes it hard to ensure that optimal conditions and dimensions are obtained (Cocco et al., 2014).

Traditionally the preliminary design of processes has been done by the experiments on a lab scale. The execution of experiments of CFB reactors can be both

expensive and not necessarily applicable since the scale-up processes of a fluidized bed reactor are difficult and complex. The extrapolation from lab-scale to industrial size is unreliable, especially when the Fluidized Bed Reactor (FBR) involves a reaction (Kunii & Levenspiel, 1991). Over the last decades, the possibility of simulating processes has been under constant development, compared to the traditional approach with experiments. Moreover, as computational power and knowledge increase, making accurate designs through simulations increases.

The fluidized bed technology has a wide range of applications in the process industry. The upward flow of a fluid through a bed of solid particles is a technique that results in an efficient heat and mass transfer and generally offers the process a stable production. However, due to the complexity of the flow pattern and the flow hydrodynamics within the gas-solid multiphase, the challenge of using a fluidized bed reactor rests in the design.

The current work aims to design a medium-scale chlorination reactor for producing a stream of AlCl3 that may later be converted into pure aluminum. First, the basic geometry and the size of the reactor specifications are figured out for suitable hydrodynamics based on the available gas-solid fluidization theories. Then, the design and operation of the reactor are evaluated and analyzed by the CFD simulations for actual operating and process conditions.

As the first step of the study, a circulating fluidized bed reactor (CFBR) preliminary mechanical design is completed using SOLIDWORKS®. The reactor model is then simulated/optimized with the use of CFD software called Barracuda VR® version 17.4.

Alumina chlorination is an aggressive exothermic reaction that occurs at higher temperatures (~700°C) (Bjarte, 2018), and the Cl_2 and $AlCl_3$ as a reactant and product are highly corrosive. Therefore the specification of material and the cooling system are essential parts of the design process. However, these are not considered within the scope of the current study.

2 Fluidization Process

Several variables affect the regimes in a fluidized bed; among them are the fluid properties of particles and fluid included in the process. Different regimes can categorize the behavior of the system. Generally, at the low velocity of the fluid, the bed of particles is stagnant, and flowing fluid passes through the void spaces of the particles. By rising velocity above minimum fluidization condition, the system's behavior depends on which kind of interface we have. In liquid-solid systems, a velocity above minimum fluidization gives a smooth expansion of the bed. However, in gas-solid systems, having a velocity above minimum fluidization velocity causes the expansion of the bed.

Further increase of the superficial gas velocity causes bubbles and movement of particles to go stronger. As a result, the bed height remains the same as it was at minimum fluidization condition. This regime is known as a bubbling fluidized bed (Kunii & Levenspiel, 1991).

2.1 Industrial application

The fluidized bed process has a long history in the industry. The first commercial process was introduced in the 1920s with the advent of the Winkler coal gasifier in Germany. Further, that produced high-octane gasoline by fluidized catalytic cracking units (FCCUs) in the 1940s (Cocco et al., 2014). After that, in the United States, it was suggested to use natural gas instead of petroleum fractions to produce gasoline with the fluidized bed. From the first attempts to use the fluidized bed in industry and until now, many processes have been changed and improved; thus, the range of applications has been raised. This is because of the usefulness of fluidized beds in process operation, especially for uniform temperature requirements for sensitive reactions (Kunii & Levenspiel, 1991).

Heat exchangers are an example of an application of fluidized beds due to their high rate of heat transport and uniform temperature. An example of a process that needs a high heat transfer rate is producing alloy with specific properties, a quench, and a tempering process (Liu et al., 2020). For this purpose, the utilization of a fluidized bed is often seen as a solution. Solidification of melt to produce granules is another application of fluidized bed in industry and is based on spraying molten urea by falling through a tower and passing cold air upward to solidify droplets and form granules. Another practical application is coating solids with plastic by suspending plastic particles through the air to collide a hot metal with a higher temperature than the melting point of plastic and perform coating it with plastic. Drying solids as a dryer for wet particles through hot gas is widely used to apply fluidized beds since it has a large capacity with low construction cost, high thermal efficiency, and easy operability (Chandran et al., 1990). In addition to the applications above, fluidized beds have many useful and extensive commercial applications based on physical operations. Among them are adsorption, transportation, mixing of fine powders, and chemical operations like carbonization, solid catalyzed reaction, and combustion (Kunii & Levenspiel, 1991).

2.2 Fluidized Bed Pros and Cons

Fluidized beds have three main advantages (Ahmadpour Samani et al., 2020). The first is the excellent heat and mass transfer between solids and fluids, leading to the low surface area needed for heat exchangers within the fluidized bed. The second one is the easy movement of solids, like fluid causes continuous operation and rapid mixing to the isothermal condition that avoids abrupt

temperature changes, making it a safe and stable method. The third one is the ability to process solids with a wide range of size distributions. As a result, they are suitable for all scale operations and have high gas and solid throughput.

There are some challenges in designing and building fluidized beds as they have inherent difficulties scaling up from lab-scale experiments. They also tend to have erosion because of the collision of particles into surfaces of vessels and pipes. The substantial losses can raise operating costs, especially if they are expensive catalysts. In addition, the rapid mixing and attrition of solids make non-uniform residence time for solids. Managing the giant bubbles in mass transfer cases are another challenge for fluidized bed (Cocco et al., 2014).

Despite these mentioned challenges, the benefits of the fluidizing bed raise interest in the widespread industrial application making it a proper method in many industrial processing operations.

3 Reactor Design

Based on the given chlorination reaction (Figure 1), the following steps have been taken to design an industrial CFBR for alumina chlorination, classifying them into six different categories as 1) theoretical calculations, 2) fluidization regime selection, 3) CPFD simulations, 4) design optimization, 5) corrosion analysis and material selection, and 6) mechanical design.

The fluid's superficial velocity directly affects the fluidization regime and thus the reactor performances. As discussed in section 3.1.2, the favorable regime can be achieved by choosing the fluid's velocity inside the reactor based on the calculated velocities.

3.1 Theoretical Calculations

In this section, the main calculations will be discussed step by step.

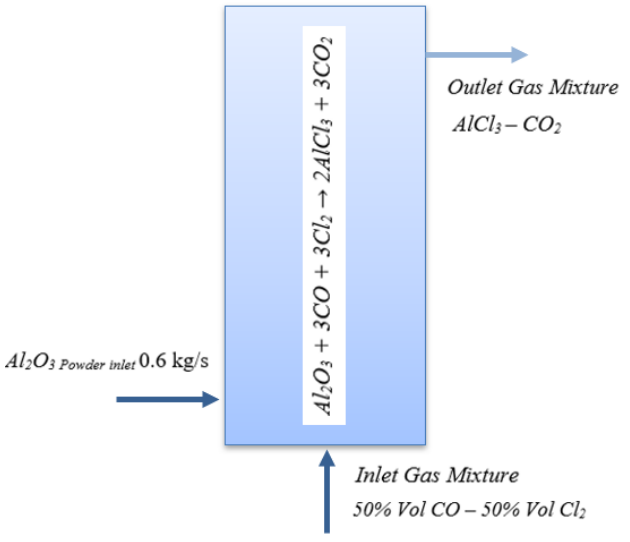

Figure 1. Illustration of the FBR

3.1.1 Mass Balance

As seen in Figure 1, the reactor should be designed for the given reaction (0.6 kg/s solid alumina with an equimolar mixture of Cl_2 and CO) at 700 ℃.

The overall reaction and mass balance are given in equations (1) and (2).

$$Al_2O_3 + 3Cl_2 + 3CO \rightarrow 2AlCl_3 + 3CO_2 \quad (1)$$

$$\dot{n}_{Al_2O_3} M_{Al_2O_3} + \dot{n}_{Cl_2} M_{Cl_2} + \dot{n}_{CO} M_{CO} = \dot{n}_{AlCl_3} M_{AlCl_3} + \dot{n}_{CO_2} M_{CO_2} \quad (2)$$

where, M is molecular weight and $\dot{n}$ is molar flow rate. Table 1 shows the calculated mass and molar flow rate for the reactants and products.

Table 1. Summarized results of the mass balance

Component	M ($\frac{g}{mole}$)	$\dot{m}$ ($\frac{kg}{s}$)	$\dot{n}$ ($\frac{mole}{s}$)
Al_2O_3	101.9	0.6	5.88
Cl_2	70.9	1.252	17.65
CO	28.01	0.494	17.65
$AlCl_3$	133.34	1.569	11.77
CO_2	44.01	0.777	17.65

3.1.2 Effect of superficial gas velocity on fluidization

There are several important velocities in a fluidized bed reactor hydrodynamics, such as minimum fluidization (u_{mf}), minimum bubbling (u_{mb}) and terminal (u_t) velocity. Although many factors affect the fluidization regime, such as solid particle Geldart classification (Kunii & Levenspiel, 1991), the fluid's superficial velocity significantly affects the bed regime. As discussed earlier, choosing the velocities below minimum fluidization velocity leads to having a fixed bed. By rising velocity above that velocity, a smooth expansion of the bed will happen accordingly. In a multiphase (gas-solid) system, bubbles are generated for velocities above minimum bubbling velocity, particles' movement is stronger, and bed height increases relatively. In the velocities above terminal velocity, fluidization will be transferred to a pneumatic transport scenario.

The given alumina sample can be categorized as Geldart A, as per its characteristic properties. Therefore, the minimum fluidization velocity can be calculated by solving the following quadratic equation:

$$\frac{1.75}{\varepsilon_{mf}^3 \, \emptyset_s}(Re)^2 + \frac{150 - (1 - \varepsilon_{mf})}{\varepsilon_{mf}^3 \, \emptyset_s^2}(Re) = \frac{d_p^3 \, \rho_g \, (\rho_s - \rho_g) g}{\mu^2} \quad (3)$$

$$Re = \frac{d_p \, u_{mf} \, \rho_g}{\mu} \quad (4)$$

where, Re is the Reynolds number, ε_{mf} is the voidage at minimum fluidization condition, $\emptyset_s$ is the solid sphericity, d_p is the average particle diameter, μ is the

fluid's dynamic viscosity, g is the acceleration gravity and ρ_g and ρ_s are fluid and solid density.

It is investigated that u_{mb}/u_{mf} is highly dependent on the weight fraction of particles smaller than 45μm (Abrahamsen & Geldart, 1980). Based on experiment on 23 different particle types and 5 different types of fluidized gases, they found the following equation to calculate the minimum bubbling velocity for fine particles as below (Kunii & Levenspiel, 1991):

$$u_{mb} = u_{mf} \frac{2300\rho_g^{0.13}\mu^{0.52}\ e^{0.72P_{45\mu m}}}{d_p^{0.8}\left(\rho_s - \rho_g\right)^{0.93}} \quad (5)$$

where, $P_{45\mu m}$ is the weight fraction of particles smaller than 45μm.

One way to calculate the terminal velocity is using Stokes law as below (Barahmand, 2021):

$$u_t = \frac{d_p^2((\rho_s - \rho_g)g}{18\mu} \quad (6)$$

Based on the parameters in Table 2, the velocities have been calculated as $u_{mf} = 0.0106\ m/s$, $u_{mb} = 0.1\ m/s$, $u_t = 0.489\ m/s$.

Table 2. Input parameters for velocity calculations

Parameter	Value	Unit
$\emptyset_s$	0.85	-
d_p	0.000098	*m*
g	9.81	*m/s²*
ρ_s	3958	*Kg/m³*
ρ_g	0.906	*Kg/m³*
μ_g	$4.45*10^{-5}$	*Pa.s*
$P_{45\mu m}$	0.0897	-

3.1.3 Reactor Diameter Calculation

The required superficial velocity (u_{req}) is equal to the inlet fluid volumetric flow rate ($\dot{V}_{in}$) divided by the cross-sectional area (which is a circle in this case). Hence, the reactor diameter (d_t) can be calculated by:

$$d_t = \left(\frac{4\dot{V}_{in}}{u_{req}\pi}\right)^{\frac{1}{2}} \quad (7)$$

In a fluidized bed reactor, the required superficial velocity can vary between the minimum bubbling velocity of 0.1 m/s and the terminal velocity of 0.489 m/s, as per the values presented in Table 2, which give values from 5.94 m to 2.47 m for reactor diameter, respectively based on the demand of the inlet gas volumetric flow rate. The flow rate of gas is calculated from the flow rate of particles set by the industrial requirements. The current study is decided based on the stoichiometry of the chlorination reaction. This means that the flow rate of gas, 2.35 m^3/s, can only be adjusted by changing the mass flow rate of particles or the number of reactors. The starting point was a somewhat arbitrary diameter, then the volumetric flow rates and the velocity were calculated stepwise. Then the three parameters were varied until an acceptable result was obtained, meaning that the velocity should be inside an acceptable range, the number of reactors was reasonable, and the diameter seemed appropriate. It ended with an internal diameter of 2.4 m, which resulted in the need for five reactors to handle 0.12 kg/s of solid particle feed in each reactor.

3.1.4 Reactor Height Calculation

An FBR has several heights with different definitions, and it is essential to differentiate between them. The fixed bed height (L_m), the height of the bubbling bed (L_f) and the height of the reactor itself (H_R) are the main ones (Kunii & Levenspiel, 1991). Determining the height depends on several factors, but an important one is the fluid's superficial velocity inside the reactor.

As discussed in section 3.1.3, the desired superficial velocity passing through the reactor can be achieved by adjusting the reactor diameter. Nevertheless, calculating the reactor height is relatively challenging. This is because many parameters, such as superficial velocity, terminal velocity, and fluidization regime, affect the reactor height simultaneously.

As shown in Figure 2, the height of a fluidized bed reactor can be divided into two main sections: the dense and lean phases. The density of solids decreases with height (Kunii & Levenspiel, 1991). The lean phase (also known as freeboard) height can be divided into two zones, where the lower part of this makes up the Transport Disengaging Height (TDH). Above the TDH is where the reactor outlet or inlet to the cyclone should be placed (Cocco et al., 2014).

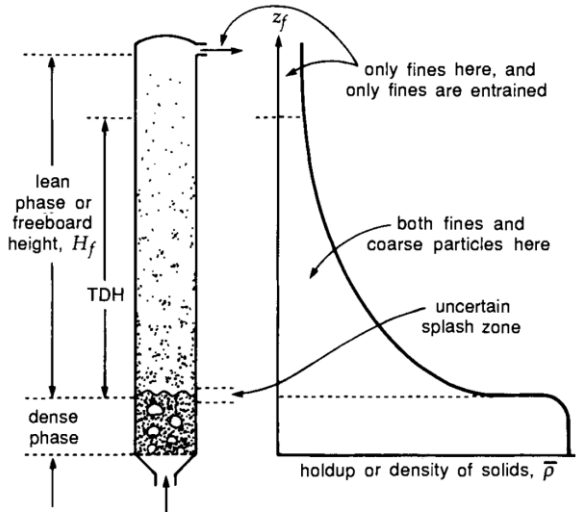

Figure 2. Different heights in a fluidized bed reactor (Kunii & Levenspiel, 1991)

The reactor height can be chosen above TDH. As a result, the minimum reactor height can be calculated by calculating the dense phase height and the TDH. The dense phase or bubbling bed height (L_f) can be calculated by series of equations ab below:

$$L_f = \frac{L_m\,(1 - \varepsilon_m)}{1 - \varepsilon_f} \quad (8)$$

where, L_m is the fixed bed height, ε_m is the voidage in a fixed bed condition and ε_f is the void fraction in a fluidized bed as a whole.

$$\varepsilon_f = \delta + (1 - \delta)\varepsilon_{mb} \quad (9)$$

where, δ is the height of bed at minimum fluidization, and ε_{mb} is the voidage at minimum fluidization condition.

$$\delta = \frac{u_o - u_{mf}}{u_b - u_{mf}} \quad (10)$$

where, u_o is the superficial gas velocity through a bed (empty vessel) and u_b is the velocity of a bubble rising through a bed.

$$u_b = u_0 - u_{mf} + u_{br} \quad (11)$$

where, u_{br} is the velocity of a bubble rising through the bed (Kunii & Levenspiel, 1991).

$$u_{br} = 0.711(g d_b)^{1/2} \quad (12)$$

$$d_b = 0.853[1 + 0.272(u_0 - u_{mf})]^{1/3}(1 + 0.0684z)^{1.21} \quad (13)$$

where, z is any height in the reactor.

Considering $u_0 = 0.175\ m/s$, $L_m = 1.6\ m$, and $\varepsilon_{mb} = 0.6$, the dense phase height will be 4.2 m. By adding 2.5 m as TDH according to Figure 3, the acceptable height for the reactor will be almost 7 meters. In the case of using an internal cyclone or other consideration, higher values can be chosen.

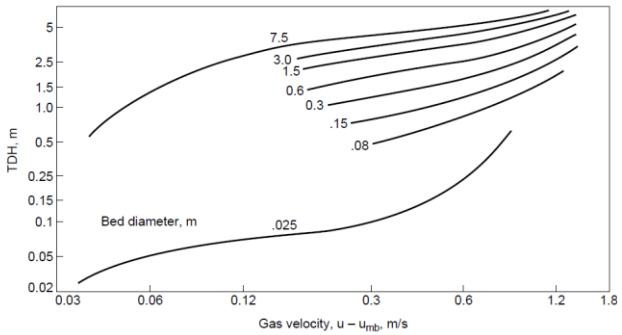

Figure 3. Estimating TDH (Perry, 1950)

4 CPFD Simulation and the Results

The CPFD simulations are based on the particle size distribution. Although in the theoretical calculation in section 3, the average particle size has been used to calculate u_{mf} and u_{mb}. Based on these theoretical values, the required superficial gas velocity inside the fluidized bed reactor is estimated. This value is then fed into the CFD simulations as one of the inputs, and more sophisticated calculations are done with CFD to study the hydrodynamics of the bed with the entire distribution of particles. The reaction kinetics are based on an isothermal condition at 700℃ (Barahmand et al., 2021b). The activation temperature and pre-exponential factor in the Arrhenius equation are 4000 K and 4583 L.mol−1s−1 for a second-order reaction. As the first step, a preliminary reactor height of 15 meters was selected as an initial estimate to prevent particle escape through the exit through the top of the reactor. As shown in Figure 4, by visual observation and studying the particle mass flow rate through the reactor, CPFD simulation shows that the maximum height particles can achieve at steady-state is around 10 meters, which are slightly higher than the calculated value of 7 m section 3.1.4. This may happen because of the model uncertainties (Barahmand et al., 2021a). However, the cylindrical reactor height selected is sufficient enough to contain the particles once it reaches steady-state.

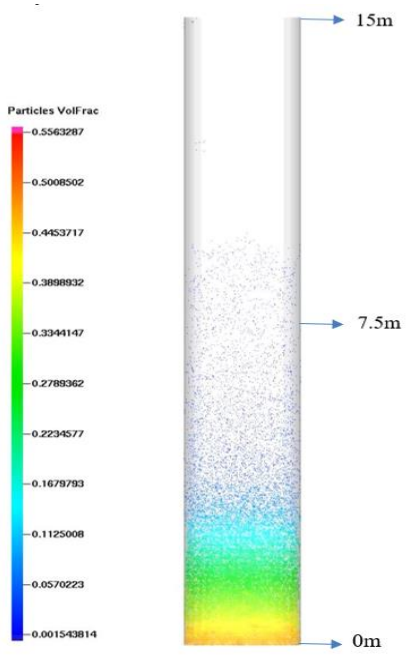

Figure 4. Bed height at the steady-state

The alumina chlorination is an exothermic and fast reaction. Due to the low reaction time, the residence time for particles could be lower as well. Based on the transient barracuda simulations, the reactor is predicted to be stabilized in around two minutes of operational time. Figure 5 shows the variation of the $AlCl_3$ and CO_2 produced at the reactor based on the reaction (1).

Based on the reaction stoichiometry, the mole fraction of produced aluminum chloride and carbon dioxide at steady-state should be 2:3, equivalent to 2:1 mass fraction. Therefore, at the steady-state, the average mass flow rate of $AlCl_3$ and CO_2 have been calculated as 0.381 kg/s and 0.188 kg/s, respectively.

The chlorination product composition in the outlet has been calculated and compared with the results based on theoretical manual calculation, process simulations (Aspen Plus®), and CFD simulations (see Table 3).

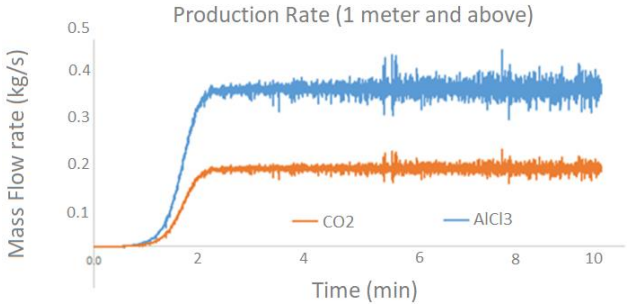

Figure 5. Product's mass flow rate at the outlet

Table 3. Component mass flow rates (kg/s) at the outlet

	Mass Flow Rates (kg/s)		
	CPFD Simulation (Barracuda®)	Theoretical	Process simulations (Aspen Plus®)
$AlCl_3$	0.381	0.314	0.313
CO_2	0.188	0.155	0.155
CO	0.00145	0	0.00021
Cl_2	5×10^{-7}	0	0.00055

By changing the fluid's superficial velocity from minimum bubbling to higher velocities, the reactor experiences different regimes. As the second step, the effect of the superficial velocity inside the reactor on the reaction and hydrodynamics has been studied. Table 4 shows the aluminum chloride ($AlCl_3$) production rate is low (minimum bubbling), medium, and high (terminal) velocities.

Table 4. Effect of the fluid velocity on $AlCl_3$ production

Velocity *m/s*	Particles Inflow Rate (kg/s)	Number of Reactors[1]	Total Production Rate (kg/s)
0.1	0.12	5	1.9040
0.3	0.35	1.7	1.9409
0.52	0.6	1	1.9862

As shown in Table 4, a higher production (around 1%) can be achieved by increasing the velocity, but the number of reactors is reduced from 5 to 1. Therefore, in the next step, the design will be optimized based on the turbulent regime.

5 Design Optimization

The reactor has been optimized based on the turbulent regime (fast fluidization), with four internal cyclones designed based on the Lapple cyclone design (Barahmand et al., 2021a). The reactor diameter has been kept the same as before (2.4 m).

[1] To reach 0.6 kg/s.

The inlet of the cyclones has a height of 7 meters which gives the reactor height 9.7 m. The cyclones have been designed for 99% efficiency, and the cyclones' arrangement has been chosen based on a Gasifier design reported in the Barracuda® training material (*Barracuda User Manual*, 2021). Figure 6 shows the particle distribution in the reactor.

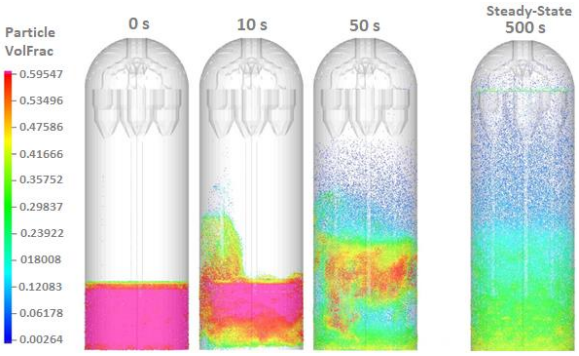

Figure 6. Simulated alumina chlorination reactor (fast fluidized bed with four internal cyclones)

6 Mechanical Design and the Material Selection

Operating conditions in this application (700°C and 50% dry-chlorine) are challenging to handle. A very high temperature decreases the resistance of the metals, and a high concentration of chlorine at the given temperature is insanely corrosive (Chang & Wei, 1991). Most of the strong alloys can tolerate just 2% of chlorine in long-term operations. Figure 7 provides a simple guide to select the different alloys for dry chlorine conditions and indicates design parameters for internals such as tubes in heat exchangers and vessel components or pipes (Davies, 2018). The corrosion rates are based on short-term tests and should not be considered a solution in long-term operations or higher concentrations.

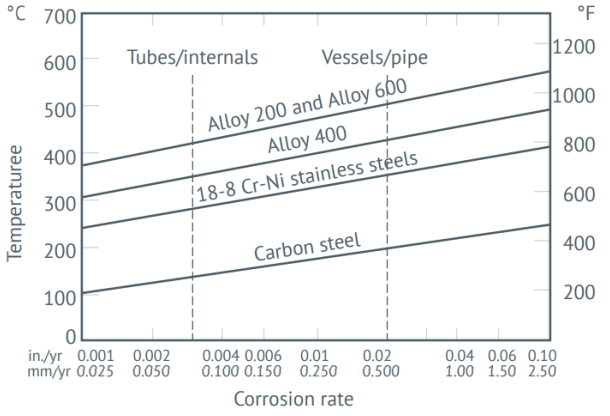

Figure 7. Upper design limits for various alloys in dry chlorine (Davies, 2018)

Some of the alloys, specifically nickel-base ones, are more resistant in these kinds of conditions. However, it should not be forgotten that all these experiments and results have been tested in dilute chlorine, which is not the case in a real-life application.

As seen in Figure 8, HAYNES® 214 alloy shows remarkable resistance to corrosion in high-temperature chlorine. Test results are shown for less than 500 hours of contact in a flowing gas mixture of Ar + 20% O_2 + 0.25% Cl_2. Note that the metal loss showed by HAYNES® 214 alloys is very low compared to other alloys tested. Another alternative to this is INCONEL® alloy 600 (*HAYNES® 214® ALLOY*, 2008).

In many cases, constructing a massive reactor with these materials is not economical for design and cost. A carbon steel reactor with special refractory linings, as an example, should be replaced in industrial-scale design.

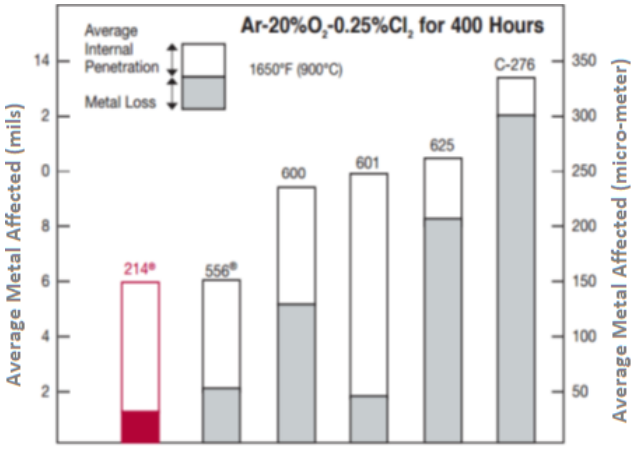

Figure 8. Resistance to chlorine corrosion (*HAYNES® 214® ALLOY*, 2008)

Using the process data, the overall mechanical design for the reactor (Figure 9) has been used to draw the 3D model of the reactor (Figure 10). As discussed earlier, the preferred material for the reactor itself is a combination of carbon steel and refractory lining. Despite being cost-beneficial, this method has more operational safety because of the high temperature. Therefore, two layers of semi-silica brick and high-alumina refractory (150 mm each) have been chosen for the lining. The lining's thickness and materials can be modified during detail engineering.

Figure 11 shows the four internal parallel cyclone's arrangement in the fast fluidized bed reactor. Figure 12 illustrates the top and bottom views of the reactor both internally and externally. For the gas distribution system, a perforated (Kunii & Levenspiel, 1991) pipe sparger mechanism (Kulkarni et al., 2009) has been designed and located at the bottom of the reactor.

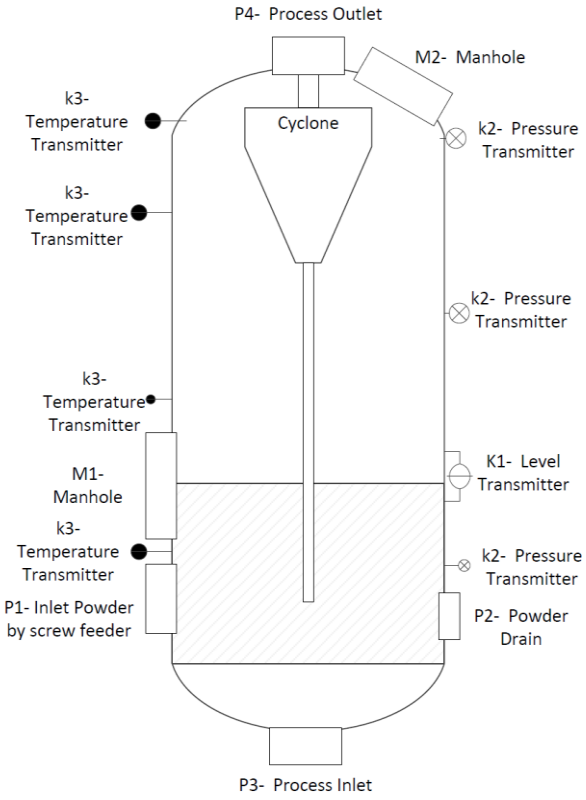

Figure 9. Overall assembly design of the reactor

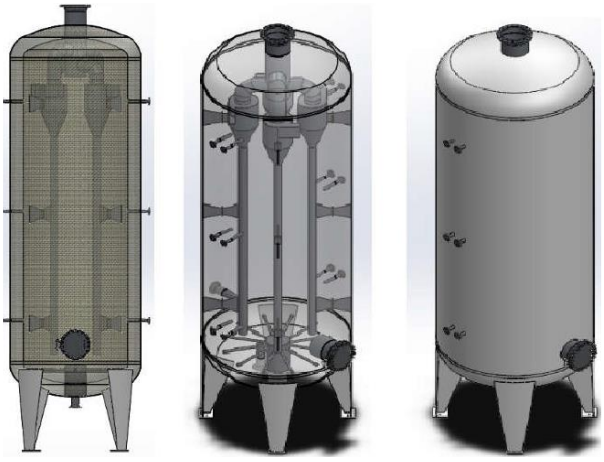

Figure 10. Reactor general assembly

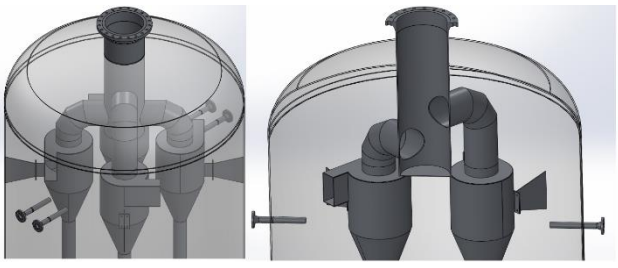

Figure 11. The cyclones arrangement

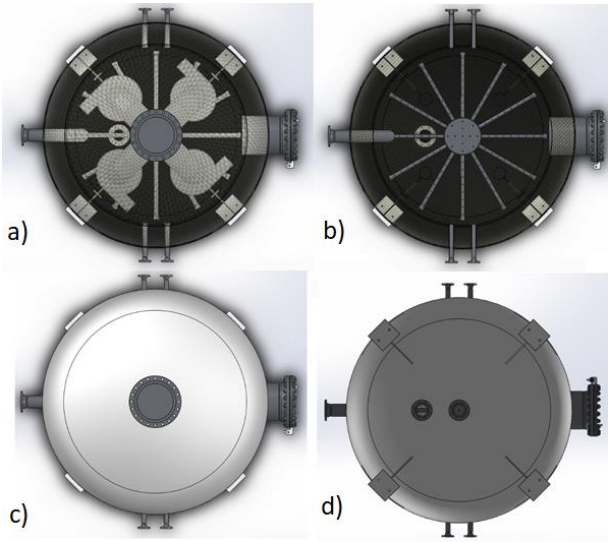

Figure 12. a) Internal top view, b) internal bottom view, c) external top view, and d) external bottom view

7 Conclusion and future development

The present study results have been evaluated and implied that the present approach can be a practical solution for industrial aluminum production with lower environmental effects as CO_2 produced from the process can be separated directly after the crystallization of $AlCl_3$. It can be concluded that the promising results suggest continuing the work and research towards implementing a real-life industrial-scale reactor. It is crucial to validate the CFD simulation data with a lab-scale experimental unit as future work. However, the results have been verified within the considered design parameters with theoretical methods and Aspen Plus® simulations. The overall internal diameter and height of the reactor are 2.4 m and 8 m, respectively. The circulation unit includes four parallel cyclones with a 0.45 m diameter.

References

A. Abrahamsen and D Geldart. Behavior of gas-fluidized beds of fine powders part I. Homogeneous expansion. *Powder Technology*, *26*(1), 35–46, 1980. doi:10.1016/0032-5910(80)85005-4

N. Ahmadpour Samani, C, Jayarathna, and L.A.Tokheim. Fluidized bed calcination of cement raw meal: Laboratory experiments and CPFD simulations. *In Proceedings - 61st SIMS Conference on Simulation and Modelling SIMS 2020*, 2020. doi:10.3384/ecp20176407

Z. Barahmand. *Design of an Industrial Chlorination Reactor Using CPFD Simulations*, Master Thesis, University of South-Eastern Norway, 2021.

Z. Barahmand, C. Jayarathna, and C. Ratnayake. Sensitivity and uncertainty analysis in a fluidized bed reactor modeling. *In Proceedings - 1st SIMS EUROSIM Conference on Modelling and Simulation*, Finland, 2021a.

Z. Barahmand, C. Jayarathna, and C. Ratnayake. The effect of alumina impurities on chlorination in a fluidized bed reactor: A CPFD study. *In Proceedings - 1st SIMS EUROSIM Conference on Modelling and Simulation*, Finland, 2021b.

Barracuda User Manual. CPFD Software, 2021. https://cpfd-software.com/

Ø. Bjarte. *Carbochlorination routes in production of Al*, pages 57, SINTEF Industry, 2018.

A. N. Chandran, S. S. Rao, and Y. B. G. Varma. Fluidized bed drying of solids. *AIChE Journal*, *36*(1), 29–38, 1990. doi:10.1002/aic.690360106

Y. N. Chang and F. I. Wei. High-temperature chlorine corrosion of metals and alloys. *Journal of Materials Science*, *26*(14), 3693–3698, 1991. doi: 10.1007/BF01184958

R. Cocco, S. Karri, and T. Knowlton. Introduction to Fluidization. *Chemical Engineering Progress*, *110*, 21–29, 2014.

M. Davies. *Alloy selection for service in chlorine, hydrogen chloride and hydrochloric acid*. Nickel Institute, 2018.

HAYNES® 214® ALLOY. Haynes International, Inc. 2008. haynes.ch/doc/haynes/214_h3008.pdf

A. V. Kulkarni, S. V. Badgandi, and J. B. Joshi. Design of ring and spider-type spargers for bubble column reactor: Experimental measurements and CFD simulation of flow and weeping. *Chemical Engineering Research and Design*, *87*(12), 1612–1630, 2009. doi:10.1016/j.cherd.2009.06.003

D. Kunii and O. Levenspiel. *Fluidization Engineering*. Butterworth-Heinemann, 1991.

Z. Liu, G. Wang, and J. Yi. Study on heat transfer behaviors between Al-Mg-Si alloy and die material at different contact conditions based on inverse heat conduction algorithm. *Journal of Materials Research and Technology*, *9*(2), 1918–1928, 2020. doi:10.1016/j.jmrt.2019.12.024

National Fuels and Energy Conservation Act. S. 2176, U.S. Government Printing Office, 1973.

J. H. Perry. *Chemical Engineers' Handbook* (Third Edition). McGraw-Hill, New York, 1950.

Y. K. Rao and M. K. Soleiman. *Alumina chlorination*. United States Patent No. US4565674A, 1986.

M. A. Rhamdhani, M. Dewan, G. Brooks, B. Monaghan, and L. Prentice. Alternative Al Production Methods: Part 1. A Review. *Mineral Processing and Extractive Metallurgy IMM Transactions Section C*, *122*, 87–104, 2013.

Survey of potential processes for the manufacture of aluminium, ANL/OEPM-79-4. Little , D. Arthur, Inc., Cambridge, MA, USA, 1979. doi:10.2172/5669730

J. Thonstad. *Aluminium Electrolysis: Fundamentals of the Hall-Héroult Process*. Aluminium-Verlag, 2001.